Journal of Inflammation Research

Dovepress
Taylor & Francis Group

Open Access Full Text Article

ORIGINAL RESEARCH

Integrating Bulk and Single-Cell Transcriptomic Data to Identify Ferroptosis-Associated Inflammatory Gene in Alzheimer's Disease

Huiqin Zhou[1–3,*], Yunjia Peng[2,3,*], Xinhua Huo[2,3], Bingqing Li[2,3], Huasheng Liu[4], Jian Wang[3,5], Gaihua Zhang[1]

[1]College of Life Sciences, Hunan Normal University, Changsha, People's Republic of China; [2]Hunan Guangxiu Hospital, Hunan Normal University, Changsha, People's Republic of China; [3]National Engineering Center of Human Stem Cell, Changsha, People's Republic of China; [4]Department of Radiology, The Third Xiangya Hospital, Central South University, Changsha, People's Republic of China; [5]The Institute of Reproduction and Stem Cell Engineering, School of Basic Medical Sciences, Central South University, Changsha, People's Republic of China

*These authors contributed equally to this work

Correspondence: Gaihua Zhang, The National and Local Joint Engineering Laboratory of Animal Peptide Drug Development, College of Life Sciences, Hunan Normal University, Changsha, China. FuRong Laboratory, Changsha, Hunan, 410078, People's Republic of China, Email ghzhang@hunnu.edu.cn; Jian Wang, The Institute of Reproduction and Stem Cell Engineering, School of Basic Medical Sciences, Central South University, Changsha, 410006, People's Republic of China, Email 205106@csu.edu.cn

Background: Ferroptosis is a form of programmed cell death triggered by iron-dependent lipid peroxidation, characterized by iron accumulation and elevated reactive oxygen species (ROS), leading to cell membrane damage. It is associated with a variety of diseases. However, the cellular and molecular links between ferroptosis, immune inflammation, and the brain-peripheral blood axis in Alzheimer's disease (AD) remain unclear.

Methods: We integrated bulk RNA-seq data from AD brain tissue and peripheral blood and refined the screening of AD candidate genes through differential gene expression analysis, weighted gene co-expression network analysis (WGCNA), and other approaches. Additionally, we analyzed single-cell RNA-seq (scRNA-seq) data from AD patients' brain tissue and peripheral blood, combined with scRNA-seq data from experimental autoimmune encephalomyelitis (EAE) mouse brain tissue. This enabled us to explore AD-related molecular mechanisms from a cell-type-specific perspective. Finally, candidate genes were validated in ferroptosis models using reverse transcription quantitative PCR (RT-qPCR) and immunofluorescence methods.

Results: Bulk RNA-seq analysis identified SLC11A1, an inflammatory gene associated with AD. Single-cell RNA-seq analysis further revealed that SLC11A1 expression was significantly elevated in the pro-inflammatory (M1-type) microglia and peripheral blood monocytes in AD. Moreover, we identified a microglial subpopulation in AD M1-type microglia that was highly associated with ferroptosis. This subpopulation simultaneously expressed characteristic markers of peripheral blood monocytes, suggesting that these cells may originate from peripheral blood monocytes, thereby triggering neuroinflammation through the ferroptosis pathway. Cell experiments confirmed that SLC11A1 was significantly upregulated in inflammatory microglia induced by ferroptosis.

Conclusion: This study reveals the key role of SLC11A1 in AD, particularly in the context of ferroptosis and immune inflammation. It provides a novel molecular mechanistic perspective and offers potential targets for future therapeutic strategies.

Keywords: Alzheimer's disease, single-cell RNA sequencing, microglia, ferroptosis, SLC11A1

Introduction

Alzheimer's disease (AD) is a common neurodegenerative disease in the elderly population, with an estimated 55 million people worldwide affected by AD, and this number is expected to increase to 139 million by the mid-21st century.[1] Chronic inflammation is considered a significant factor in the development of AD. In the brains of AD patients, long-term inflammation is often observed, including the activation of microglia and an increase in inflammatory factors. Recent studies have shown that ferroptosis mediates inflammation in AD.[2] Ferroptosis is an identified form of cell death

Received: 22 September 2024
Accepted: 31 January 2025
Published: 10 February 2025

driven by intracellular phospholipid peroxidation. Accumulating evidence suggests that ferroptosis plays a significant role in inflammation, with several antioxidants acting as ferroptosis inhibitors and demonstrating anti-inflammatory effects in experimental models of various diseases.[3] Furthermore, emerging evidence suggests that immune cell infiltration, particularly involving microglia and peripheral immune cells, plays a crucial role in the inflammatory response associated with AD progression. Notably, peripheral blood monocytes can infiltrate the brain parenchyma, where they differentiate into macrophage-like cells with features resembling those of microglia.[4,5] However, the precise role of these macrophage-like cells in the inflammatory environment of AD remains a subject of considerable debate. Understanding the relevant molecules involved in immune cell infiltration and their interactions within the AD brain microenvironment is crucial for elucidating the mechanisms underlying disease progression and identifying potential therapeutic targets aimed at modulating the immune response to mitigate neuroinflammation in AD.

The SLC11 family (Solute Carrier 11), also known as the NRAMP family (Natural resistance-associated macrophage protein), is a class of transmembrane ion transporter protein family. This family includes two main members, SLC11A1 and SLC11A2.[6] Past studies have indicated the association of the SLC11 family with tuberculosis and autoimmune diseases.[7,8] Although some studies have reported low association between the polymorphisms of these two molecules and AD,[9] researchers have begun to re-examine their roles in neurodegenerative diseases with the development of transcriptome sequencing technology. For instance, increased expression of SLC11A2 in the substantia nigra of Parkinson's disease (PD) patients has been found to promote iron accumulation, which initiates ferroptosis by driving iron-dependent lipid peroxidation. This process leads to oxidative stress, protein aggregation, and neuronal death, contributing to the neurodegenerative progression observed in PD.[10] Additionally, elevated expression of SLC11A1 has been observed in the hippocampus of AD models across species.[11,12] However, its specific function in the brain and peripheral blood environment of AD remains poorly understood due to the complexity and heterogeneity of the cell populations involved, which underscores the need to integrate single-cell RNA sequencing (scRNA-seq) data for a more precise and comprehensive analysis. scRNA-seq provides a comprehensive and detailed analysis of individual cells, allowing researchers to discern subtle differences in cell populations and identify rare cell types that may play crucial roles in disease pathogenesis. Therefore, combining scRNA-seq and bulk RNA-seq data to explore molecular compositional changes in related cells of AD has emerged as a promising direction. This not only improves the accuracy and efficiency of the discovery of molecular biomarkers for AD, but also has important implications for linking cell function with gene expression.

In this study, we integrated AD brain tissues and peripheral blood bulk RNA-seq data, using methods like differential gene expression analysis and weighted gene co-expression network analysis (WGCNA) to identify AD candidate genes. scRNA-seq from AD patients and experimental autoimmune encephalomyelitis (EAE) mice was analyzed to elucidate connections among different cell types. Pseudotime analysis simulated expression changes during cell differentiation, while CellChat analyzed signaling pathways. Candidate genes were verified using transcription quantitative polymerase chain reaction (RT-qPCR), immunofluorescence and receiver operating characteristic (ROC) analysis, and diagnostic efficacy was assessed with decision curve analysis (DCA). The bulk RNA-seq analysis results revealed that SLC11A1 is an inflammation-related gene associated with AD. scRNA-seq further demonstrated that SLC11A1 expression was significantly upregulated in M1-type microglia and peripheral blood monocytes in AD. Additionally, we identified a ferroptosis-associated subpopulation in AD M1-type microglia, which simultaneously expressed characteristic markers of peripheral blood monocytes. This suggested that these cells may originate from peripheral blood monocytes and trigger neuroinflammation through the ferroptosis pathway. Finally, cell experiments confirmed the upregulation of SLC11A1 in inflammatory microglia induced by ferroptosis, suggesting that SLC11A1 may play an important role in mediating the inflammatory response associated with ferroptosis in microglial cells.

Materials and Methods

Data Collection

The datasets for this study were obtained from the Gene Expression Omnibus (GEO) database. This includes four bulk RNA-seq transcriptome datasets relevant to AD: GSE29378, GSE63060, GSE63061, and GSE33000. Additionally, the

study incorporates three AD-related scRNA-seq datasets: GSE175814, GSE188545, and GSE168522. Furthermore, we also included the scRNA-seq dataset GSE199460 w ith EAE, enriching the research resources available for understanding the molecular underpinnings of AD and related autoimmune neurological disorders. The specific information for each dataset was detailed in Table 1. Furthermore, applying a correlation score above 1 as the selection threshold, we preliminarily obtained 5351 inflammation-related genes from the Genecards database.[13]

Gene Differential Expression Analysis

The hippocampus is a crucial component of the limbic system, playing a key role in learning and memory. To investigate differentially expressed genes (DEGs) in the hippocampus between normal individuals and AD patients, we selected the GSE29378[14,15] dataset from the NCBI Gene Expression Omnibus (GEO) database. The analysis was performed using the "limma" package of R. The expression profile data were log-transformed, and genes with an adjusted p-value < 0.05 and $|\log_2 FC| > 0.5$ were considered as DEGs associated with AD. The results were visualized using the "pheatmap" package of R.

Weighted Gene Co-Expression Network Analysis

WGCNA is a systems biology method used to construct gene co-expression networks and identify gene modules significantly associated with specific phenotypes.[16] Pearson correlation analysis was used to calculate the correlation between module eigengenes (MEs) and the clinical status of the samples in the GSE29378 dataset, using the R package "WGCNA". Modules were distinguished by different colors, and the module showing the highest correlation with clinical status was selected as the key module.

Gene Ontology (GO) Annotation and Construction of the Protein-Protein Interaction (PPI) Network

GO annotation analysis was performed using the "clusterProfiler" package[17] of R to predict the potential functional roles of the selected genes in biological processes (BP), cellular components (CC), and molecular functions (MF). Simultaneously, we utilized Cytoscape (version 3.9.1) and STRING database (https://string-db.org/) to construct a PPI network and identify key molecules based on the degree values of protein-protein interactions.[18]

Immune Infiltration Analysis

The ssGSEA was utilized to analyze the differential infiltration of 26 types of immune cells between control and AD hippocampal tissues from the GSE29378 dataset. ssGSEA evaluates the activity levels of immune-related gene sets in individual samples, thereby inferring the degree of immune cell infiltration in the sample.[19] It not only considers the expression levels of individual genes but also takes into account the overall expression pattern of genes within the gene set, allowing for a more accurate assessment of immune gene set activity. We also performed a correlation analysis between the immune cells

Table 1 Details of the Datasets Used in This Study

Diseases	GEO Series	GPL Platform	Transcriptome Data Type	Region	Control Group Size	Disease Group Size
AD	GSE29378	GPL6947	Bulk RNA-seq	Hippocampus	32	31
	GSE63060	GPL6947	Bulk RNA-seq	Peripheral Blood	104	MCI:80; AD:145
	GSE63061	GPL10558	Bulk RNA-seq	Peripheral Blood	134	MCI:109; AD:139
	GSE175814	GPL24676	scRNA-seq	Hippocampus	2	2
	GSE188545	GPL24676	scRNA-seq	Middle Temporal Gyrus	6	6
	GSE168522	GPL11154	scRNA-seq	Peripheral Blood	2	4
	GSE33000	GPL4372	Bulk RNA-seq	Prefrontal Cortex	157	310
EAE	GSE199460	GPL24247	scRNA-seq	Total Brain (mouse)	6	5

Abbreviations: AD, Alzheimer's disease; EAE, experimental autoimmune encephalomyelitis; MCI, mild cognitive impairment.

with significantly different infiltration and the previously selected genes, further identifying the hub genes most strongly correlated with immune cell infiltration.[20] The results were further visualized using the "ggplot2" and "corrplot" R packages.

Identification of Candidate Genes in Peripheral Blood for AD and Analysis of Their Association With AD Pathology

To explore whether the candidate genes for AD identified through screening exhibit consistent expression differences in peripheral blood, we included two AD peripheral blood expression datasets, GSE63060 and GSE63061.[21] The correlation between candidate genes and AD pathology was also analyzed, we included mice with AD pathology from the MOUSEAC database[22] for correlation analysis. The selected regions were the hippocampus and cerebral cortex, including 62 samples of Aβ pathology mice with APP and PSEN1 heterozygous mutations (HET_TASTPM and HO_TASTPM), and 30 samples of Tau pathology mice with TAU transgenes (TAU).

Gene Set Enrichment Analysis

For Gene Set Enrichment Analysis (GSEA), we utilized GSEA software (version 3.0).[23,24] The samples were divided into high-expression (≥50%) and low-expression (<50%) groups based on the expression levels of AD candidate genes. This division aimed to assess relevant pathways and molecular mechanisms. The analysis was conducted using the gene expression profile from GSE29378, with a minimum gene set size set to 5, maximum gene set size set to 5000, and 1000 permutations.

scRNA-Seq Data Processing, Pseudotime and CellChat Analysis

To analyze single-cell RNA sequencing data from AD and EAE models, we incorporated datasets GSE175814, GSE188545, GSE168522 and GSE199460.[25–27] Data were processed using the "Seurat" package in R. Cell clusters were annotated using the CellMarker database, which provides comprehensive information on cell markers, aiding in cell type identification and classification.[28] Microglia were extracted for pseudotime analysis,[29] with dimensionality reduction performed using UMAP, and trajectory inference conducted using the "learn_graph" function from the "monocle3" package. Visualization of cell differentiation trajectories and gene expression changes was achieved with the "plot_cells" and "plot_genes_in_pseudotime" functions. We also used the "CellChat" package to analyze signaling pathway networks between different cell types. For glial cells from EAE and control mice, potential ligand-receptor interactions were inferred based on receptor and ligand expression, referencing the "mouse" database from "CellChatDB". The results were visualized using the "netVisual_bubble" function.

Cell Culture

The BV2 cell line was purchased from Wuhan Pricella Biotechnology Co., Ltd. It is derived from the German DSMZ (German collection of microorganisms and cell cultures) and was obtained from a mouse brain microglial tumor. The culture medium of BV2 cells was 90% Duchenne Modified Eagle Medium (Gibco, 21331020) + 10% fetal bovine serum (Gibco, A5670701). The culture condition was 5% CO2, 37°C constant temperature incubator. Ferroptosis inducer RSL3 (Aladdin, R302648) was dissolved in DMSO, RSL3 is a chemical compound that induces ferroptosis by inhibiting the activity of glutathione peroxidase 4 (GPX4), leading to the accumulation of intracellular lipid peroxides.[30] And FeSO4 (Sigma-Aldrich, F8633) was dissolved in PBS. Based on a previous study,[31] BV2 cells were stimulated with appropriate concentrations of RSL3 and FeSO4 to establish the model of ferroptosis-induced microglial inflammation.

Reverse Transcription Quantitative Polymerase Chain Reaction

Total RNA was extracted from BV2 cells by using Trizol (Invitrogen, 15596026CN). RNA was reverse transcribed into complementary DNA (cDNA) using a Prime ScriptTM RT Master Mix Kit with gDNA Eraser (Takara, RR047A). The mRNA level was analyzed by Lightcycler480 SYBR II real-time PCR (Roche, Penzberg, Germany) using SYBR Green. The results were analyzed using the $2^{-\Delta\Delta CT}$ method. Data were expressed as the level of mRNA of interest normalized to GAPDH mRNA level in each sample. Specific primers for GAPDH, SLC11A1, TNF-α and ACSL4 (Table 2) were generated by Sangon Biotech (Shanghai, China).

Table 2 Primer Sequences for RT-qPCR

Genes	Forward Primer (5′-3′)	Reverse Primer (5′-3′)
SLC11A1	GTGGGCTCAGATATGCAGGAA	GCGCAAACCATAGTTATCCAAGA
TNF-α	CAGGCGGTGCCTATGTCTC	CGATCACCCCGAAGTTCAGTAG
ACSL4	CCTGAGGGGCTTGAAATTCAC	GTTGGTCTACTTGGAGGAACG
GAPDH	GGAGCGAGATCCCTCCAAAAT	GGCTGTTGTCATACTTCTCATGG

Cell Counting Kit-8 (CCK-8) and Measurement of Reactive Oxygen Species (ROS) Levels

Cell viability was assessed using the CCK-8 assay (APExBIO, K2268). In brief, 100 μL of culture medium containing 5 × 10^3 cells were added to each well of a 96-well plate. After allowing the cells to adhere and stabilize, the designated drugs were added and incubated for the specified time. Subsequently, 10 μL of CCK-8 solution was added and incubated for 1 hour, followed by measuring the absorbance at 450 nm. For measuring ROS levels, in brief, 5 × 10^5 cells were seeded in a 6-well plate. After the cells adhered and stabilized, the designated drug was added and incubated for the specified time. The medium was then removed, and 1 mL of 10 μM H2DCFDA (MCE, HY-D0940) diluted in serum-free medium was added. The cells were incubated for 25 minutes, digested with trypsin, washed with PBS, and analyzed using flow cytometry. Both CCK-8 and H2DCFDA should be incubated at 37°C in the dark.

Cell Immunofluorescence

For cell immunofluorescence, in brief, cells were seeded onto coverslips placed in culture dishes, and once the cells approached confluence, the coverslips were removed and washed with PBS. The cells were then fixed with 4% paraformaldehyde (Beyotime Biotechnology, P0099) for 15 minutes, followed by PBS washing. Next, the cells were permeabilized with 0.5% Triton X-100 (Beyotime Biotechnology, P0096) at room temperature for 15 minutes and washed with PBS. Afterward, the cells were blocked with serum at room temperature for 1 hour. The blocking solution was removed, and the cells were incubated with primary antibody against SLC11A1 (diluted 1:200, CUSABIO, CSB-PA021380LA01HU) overnight at 4°C. Afterward, the secondary antibody (diluted 1:500, Proteintech, RGAR002) was applied and incubated at 37°C for 1 hour, followed by PBST washing. To stain the nuclei, DAPI was added and incubated in the dark for 5 minutes, and excess DAPI (Beyotime Biotechnology, C1006) was washed off with PBST. Finally, the cells were observed under a fluorescence confocal microscope (ZEISS, LSM 800).

Receiver Operating Characteristic Curve and Decision Curve Analysis

To further evaluate the diagnostic capability of the selected AD candidate genes, ROC curve analysis was conducted on a dataset, GSE33000.[32] This analysis was performed using the "pROC" package. In addition, DCA was carried out using the "ggDCA" package. DCA helps assess the diagnostic value of AD candidate genes in conjunction with clinical decision-making. The threshold probability ranged from 0% to 100%, reflecting various clinical decision preferences.

Statistical Analysis

The statistical analysis was conducted using R software version 4.2.2. The Wilcoxon test or *t*-test was used to analyze the significance of differences between the two groups, and Pearson's correlation coefficient was employed to determine the correlation between variables.

Results

Identification of AD-Related DEGs in Hippocampus

In order to identify DEGs in the hippocampal tissues of AD patients compared to normal controls, we utilized the hippocampal gene expression data provided by the GSE29378 dataset and performed differential gene expression analysis using the "limma" package in R. After data normalization, a total of 132 DEGs were identified, with 106 up-

regulated and 26 down-regulated. The results are depicted in the heatmap (Figure 1A), where the color red indicates higher expression levels, and blue indicates lower expression levels.

Identification of AD-Associated Module Genes and Analysis of Their Enriched Functional Pathways

After incorporating 63 samples from GSE29378, WGCNA analysis was performed. The "pick Soft Threshold" function was employed to filter power parameters ranging from 1 to 20. In order to ensure a scale-free network, the optimal soft threshold was selected as 12 (Figure 1B). A clustering dendrogram was constructed using the "cutree" dynamic and module eigengene functions, resulting in 10 modules composed of genes with similar co-expression patterns. A module-trait relationship heatmap based on Pearson correlation coefficients was generated to assess the correlation between each module and the disease (Figure 1C and D). The heatmap revealed that 1695 genes in the yellow module were significantly positively associated with AD (p-value < 0.005).

Based on WGCNA, the genes in the yellow module were positively correlated with AD. By intersecting these genes with AD upregulated genes identified from differential gene expression analysis and inflammation-related genes from the

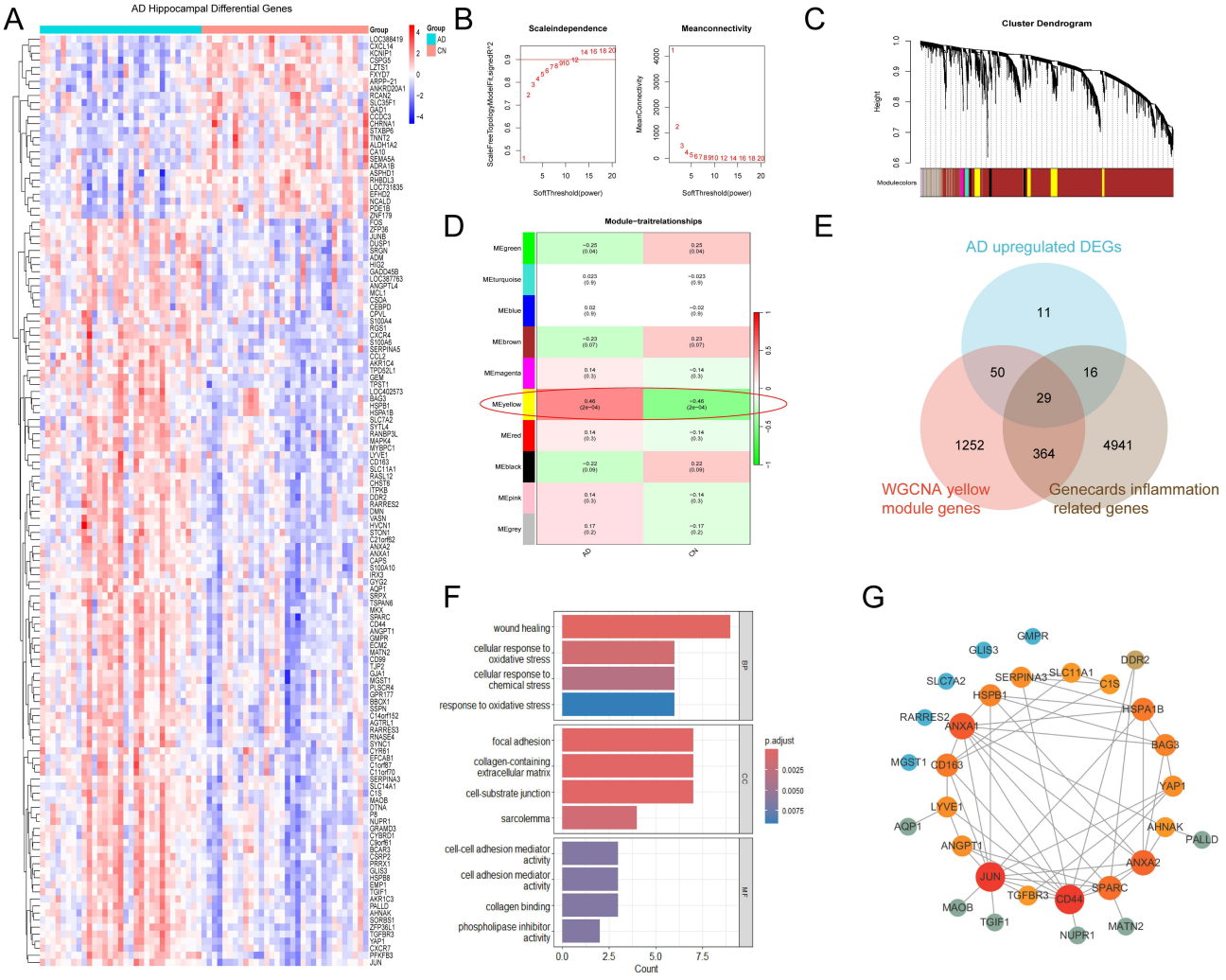

Figure 1 Analysis of AD hippocampus bulk transcriptome data. (**A**) Heatmap of hippocampal DEGs between AD and CN. (**B**) Analysis of the scale-free fitting index (β) and average connectivity under different soft-thresholding powers. (**C**) The cluster dendrogram of co-expression genes. (**D**) Correlation heatmap between 10 characteristic gene modules and clinical phenotypes. Each cell includes the correlation coefficient and p-value. (**E**) The intersection of the Venn diagram yielded AD-related inflammatory genes. (**F**) GO annotation results of genes in the AD-related inflammatory genes. (**G**) The construction of the PPI network for AD-related inflammatory genes.
Abbreviations: DEG, differentially expressed gene; GO, Gene Ontology; PPI, Protein-Protein Interaction; AD, Alzheimer's disease; CN, cognitively normal.

GeneCards database, we ultimately identified 29 genes (Figure 1E). GO enrichment analysis revealed that in the biological process category, these genes were significantly enriched in pathways related to wound healing and cellular oxidative stress. In the cellular component category, significant enrichment was observed in pathways such as focal adhesion (Figure 1F).

Construction of a PPI Network and Correlation Analysis With Immune Cells for Hub Genes Identification

A PPI network was constructed using the 29 genes previously identified, which helps in understanding disease mechanisms and identifying key molecular targets by revealing protein-protein interactions. The degree value of each molecule was calculated using the "Analyze Network" function in Cytoscape software, resulting in the selection of 17 genes with a degree value greater than 3 (Figure 1G) for correlation analysis with immune cells that exhibited significant differences in infiltration. Immune infiltration analysis of the GSE29378 dataset revealed significant differences in the infiltration of activated CD4+ T cells, central memory CD4+ T cells, monocytes/macrophages, and eosinophils between the AD and CN groups ($p < 0.001$). In AD, infiltration of activated CD4+ T cells, central memory CD4+ T cells, and monocytes/macrophages was increased, while eosinophil infiltration was decreased (Figure 2A). Correlation analysis showed that C1S was most correlated with activated CD4+ T cell infiltration ($r = 0.56$, $p < 0.001$), CD44 and C1S with central memory CD4+ T cell infiltration ($r = 0.55$, $p < 0.001$), SLC11A1 with monocyte/macrophage infiltration ($r = 0.68$, $p < 0.001$), and ANXA2 with eosinophil infiltration ($r = -0.45$, $p < 0.001$) (Figure 2B).

The Increased Expression of SLC11A1 in AD Brain Tissue Is Reflected in Peripheral Blood and Is Associated With AD Pathology

Correlation analysis was conducted on four genes (C1S, CD44, SLC11A1, ANXA2) using AD peripheral blood expression datasets GSE63060 and GSE63061. The results showed that SLC11A1 is also up-regulated in the peripheral blood of AD patients in both datasets (Figure 3A). Moreover, the expression of SLC11A1 is highly correlated with Aβ and Tau pathology in mice (Aβ: $R = 0.89$, $p < 2.2e\text{-}16$; Tau: $R = 0.76$, $p = 1.0e\text{-}6$) (Figure 3B and C). In GSEA, SLC11A1 is enriched in pathways such as JAK-STAT and antigen processing and presentation, indicating its potential role in the immune response process (Figure 3D).

SLC11A1 Was up-Regulated in AD Microglia and Peripheral Blood Monocytes

To investigate the expression of SLC11A1 in AD at the cellular level, we utilized scRNA-seq data from the GSE175814 dataset, which includes data from the hippocampal anterior cortex, and the GSE168522 dataset, which contains data from peripheral blood. Initially, we performed quality control on the GSE175814 dataset by filtering out cells with mitochondrial genome percentages greater than 5% and cells with gene counts outside the range of 200 to 2500. The data were then log-normalized and integrated using the "harmony" package, followed by batch effect removal and dimensionality reduction using UMAP, resulting in the identification of 22 distinct cell clusters. Cell annotation was performed using CellMarker, with feature genes such as ITGAM and P2RY12 for microglia, GFAP, ALDH1L1, and ATP13A4 for astrocytes, MBP and CNP for oligodendrocytes, GAD1, GAD2, and SLC32A1 for inhibitory neurons, and CUX2, NRGN, and SLC17A7 for excitatory neurons (Figure S1). Subsequently, the cells were divided into AD and CN groups to compare differences in cell composition. The analysis revealed a reduced proportion of astrocytes in the AD group, accompanied by an increase in microglia. Notably, SLC11A1 is specifically expressed in microglial cells in the brain, and its expression was significantly up-regulated (P-value < 0.001) in microglia from the AD group. This finding was also replicated in the middle temporal gyrus (Figure 4A–D; Figure S2).

To further investigate whether similar expression patterns of SLC11A1 are observed in peripheral blood cells, we analyzed the GSE168522 dataset, which provides scRNA-seq data from peripheral blood. Quality control and normalization were performed following the same standards applied to GSE175814. The cells were classified into 26 clusters, and for cell classification, we used CD19, CD38, and MS4A1 as marker genes for B cells; CD4, IL7R, and CCR7 for CD4+ T cells; CD8A and CD8B for CD8+ T cells; CD14, LYZ, S100A9, S100A8, and MS4A7 for monocytes;

 https://doi.org/10.2147/JIR.S497418

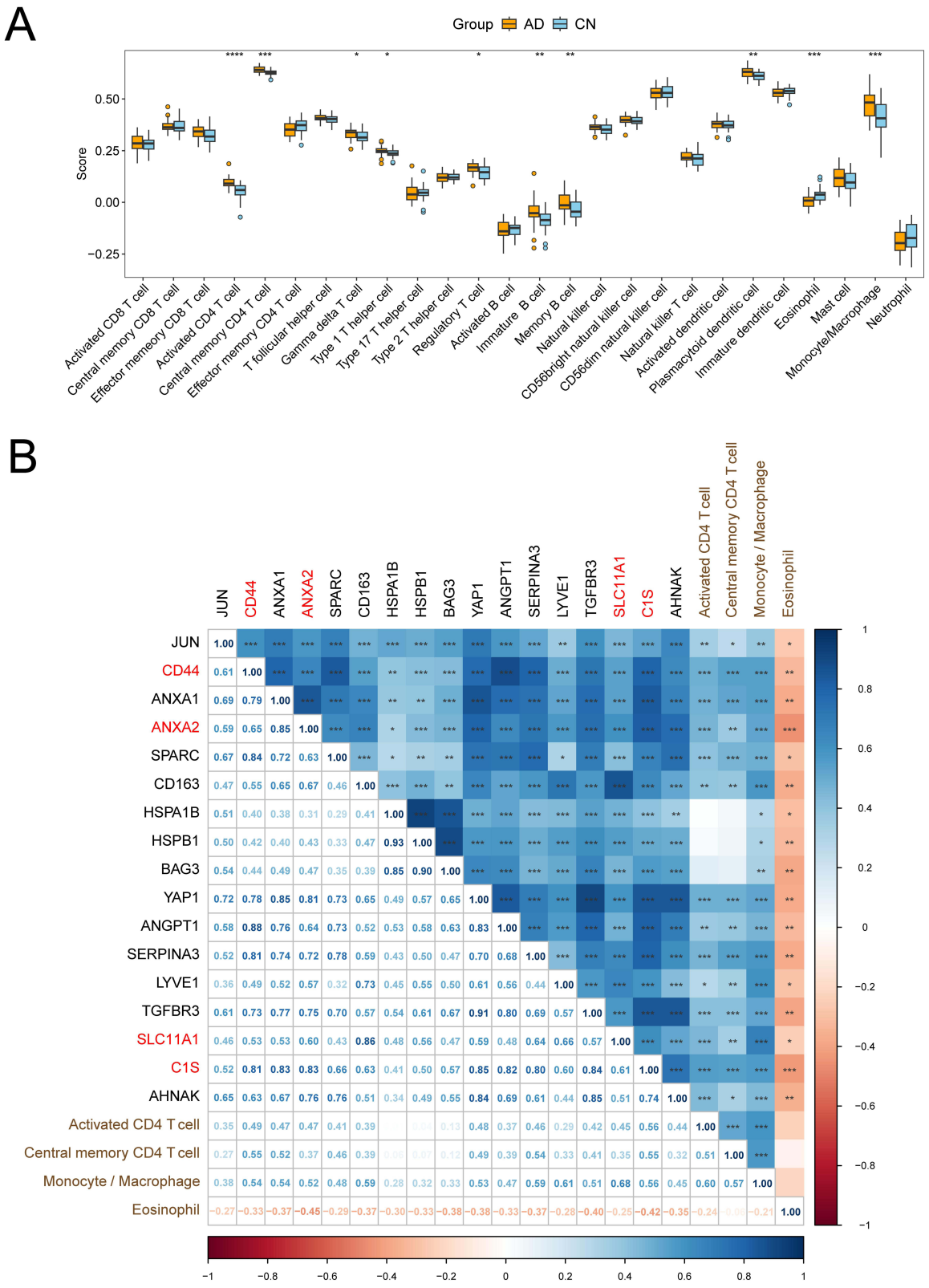

Figure 2 Immune infiltration analysis and the correlation analysis between genes and immune cells. (**A**) Differences in immune infiltration of 26 immune cells between AD and CN. (**B**) The correlation analysis between hub genes and immune cells. Blue indicates a positive correlation, while red indicates a negative correlation. The numbers represent Pearson correlation coefficients. The significance levels are denoted as *p-value < 0.05, **p-value < 0.01, and ***p-value < 0.001.
Abbreviations: AD, Alzheimer's disease; CN, cognitively normal.

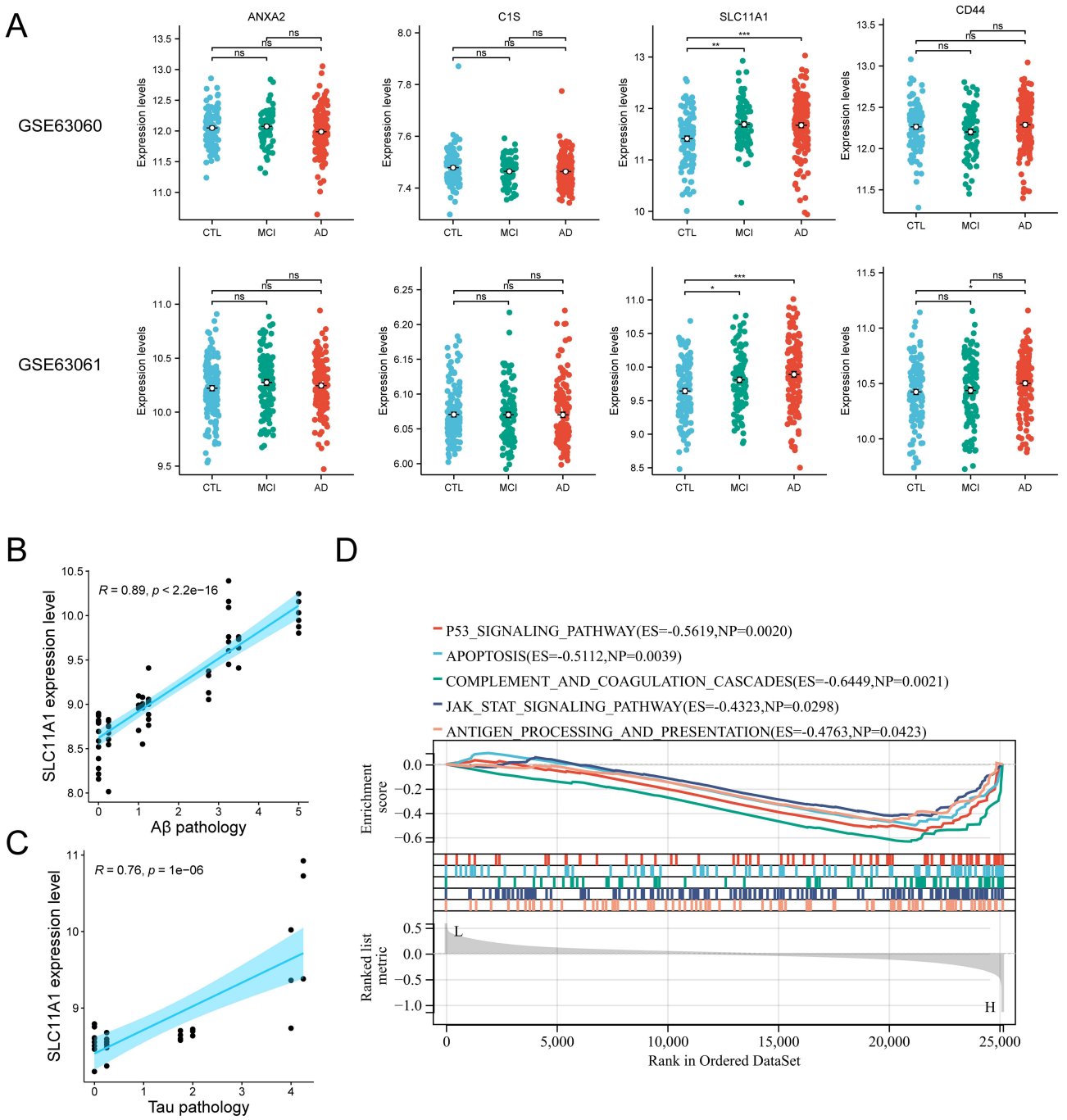

Figure 3 Differential expression of candidate genes in peripheral blood across CTL, MCI, and AD and their correlation with AD pathology. (**A**) Expression differences of four candidate genes in peripheral blood among AD, MCI, and CTL groups, significance was tested using the Wilcoxon test. (**B-C**) Correlation of SLC11A1 with Aβ and Tau pathology in AD model mice. Conduct correlation analysis using the Pearson correlation coefficient. (**D**) GSEA for SLC11A1.
Abbreviations: AD, Alzheimer's disease; CTL, control; MCI, mild cognitive impairment; GSEA, Gene Set Enrichment Analysis.

FCGR3A, CCL3, KLRB1, NCR1, GNLY, and NKG7 for NK cells; and PPBP for platelets (Figure S3). Similar to the data processing method used for the cortical samples, the cells were categorized into AD and CN groups. The results showed that SLC11A1 is specifically expressed in peripheral blood monocytes, with a significant up-regulation observed in the AD group (P-value < 0.001) (Figure 4E–G).

https://doi.org/10.2147/JIR.S497418

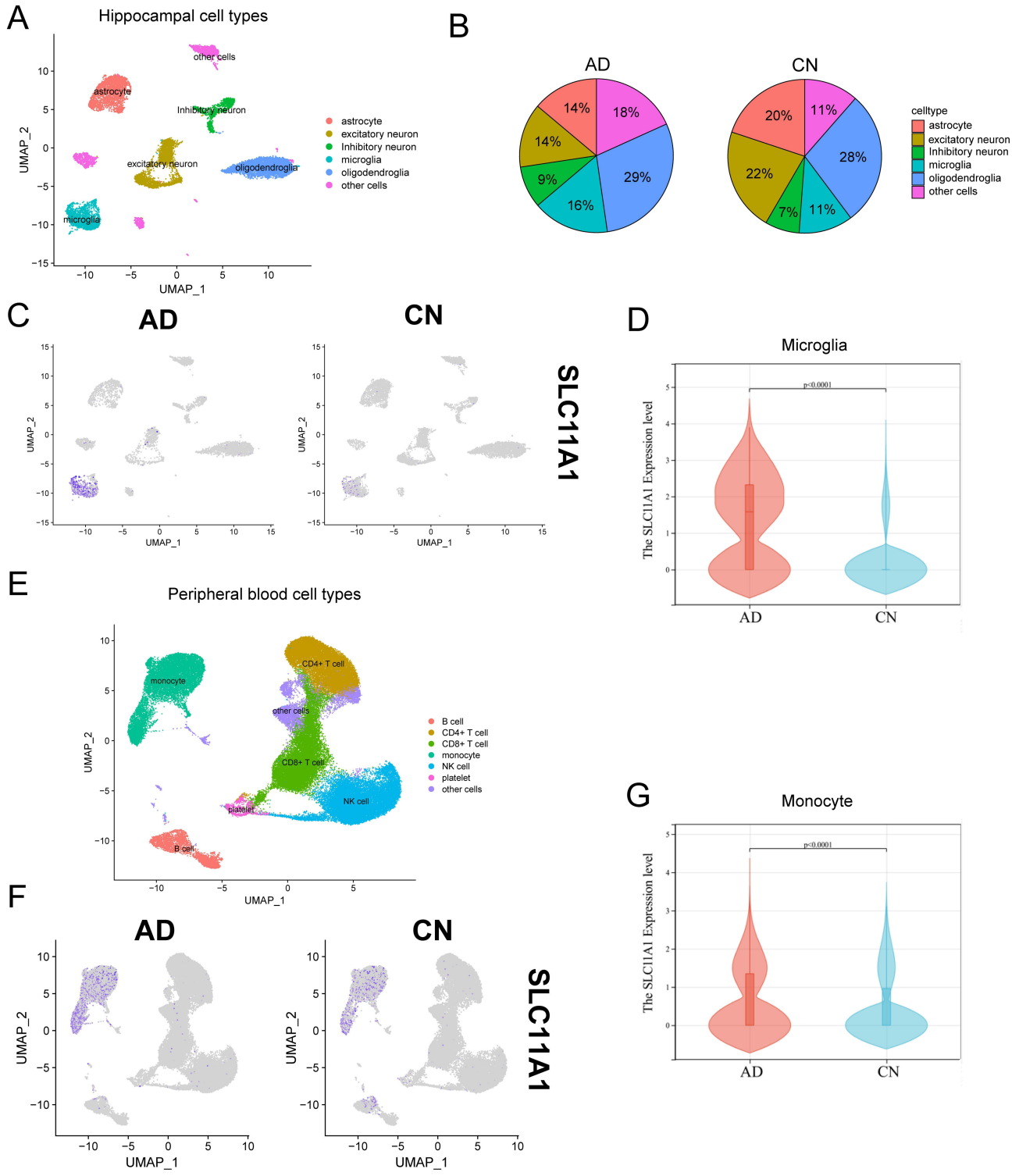

Figure 4 scRNA-seq data analysis of hippocampus and peripheral blood. (**A**) Cell distribution in hippocampus after clustering. (**B**) Proportion of cells in AD and CN groups. (**C**) Expression distribution of SLC11A1 in different hippocampus cells. (**D**) Differences in SLC11A1 expression between AD and CN groups in microglia, significance was tested using the Wilcoxon test. (**E**) Cell distribution in peripheral blood after clustering. (**F**) Expression distribution of SLC11A1 in different peripheral blood cells. (**G**) Differences in SLC11A1 expression between AD and CN groups in monocytes, significance was tested using the Wilcoxon test.
Abbreviations: AD, Alzheimer's disease; CN, cognitively normal.

Identification of a Specific M1 Microglia Subpopulation in AD Expressing SLC11A1 and Associated With Ferroptosis

Microglial cells were separately extracted from the GSE175814 dataset and subjected to re-clustering, resulting in seven distinct microglial clusters. These cells were categorized into subpopulations using M1 markers (IL18, CD86, NLRP3) and M2 markers (MRC1 [CD206], CD163), ultimately identifying Resting, Intermediate, M1, and M2 microglia subgroups (Figure 5A–C). Analysis revealed that SLC11A1 was predominantly expressed in M1 microglia in the AD group. Notably, cluster 2 contained a unique subpopulation specific to M1 microglia in the AD group, which expressed common monocyte markers such as CD14 and HLA-DPA1. This finding, along with the previously observed up-regulation of SLC11A1 in AD peripheral blood monocytes, suggests that this subpopulation may originate from peripheral blood monocytes. In addition, FTH1 and FTL1, key genes involved in iron metabolism, were also highly expressed in this subpopulation, indicating a potential link to ferroptosis (Figure 5D).

Experimental Autoimmune Encephalomyelitis (EAE) is a well-established animal model for studying brain inflammation and immune responses in the central nervous system (CNS), which induces blood-brain barrier (BBB) disruption and leads to the infiltration of peripheral immune cells into the brain parenchyma.[33] In scRNA-seq data from this model, we also identified the same microglial subpopulation, characterized by high expression of peripheral blood monocyte markers (CD14) and iron metabolism-related genes (FTH1 and FTL1). Therefore, we defined this subpopulation as infiltrating microglia, while other microglial cells were categorized as resident microglia. CellChat analysis revealed that infiltrating microglia exhibited significantly higher levels of intracellular interactions, including multiple receptor-ligand pairs associated with chemokines, TNF, and complement component 3 (C3) (Figure S4).

Pseudotime analysis further demonstrated a progression of microglial cells from a resting state to M1 polarization, with an increasing trend in SLC11A1 expression (Figure 5E and F). This suggests that the elevated expression of SLC11A1 in the AD-associated M1 microglial subpopulation may be closely linked to iron metabolism, ferroptosis, and inflammatory processes in the AD brain microenvironment.

Cellular Experiment Verification and Diagnostic Efficacy Evaluation

To determine the optimal RSL3 concentration for treating BV2 cells, we stimulated the cells with 2 μM, 5 μM, and 10 μM RSL3 for 6 hours while keeping FeSO4 at 1600 μM. Cell viability was assessed using the CCK-8 assay, leading us to select 1600 μM FeSO4 + 5 μM RSL3 as the optimal conditions (Figure 6A). Flow cytometry analysis revealed a significant increase in ROS levels in BV2 cells under this stimulation condition (Figure 6B and C). And we validated the expression levels of SLC11A1, TNF-α, and ACSL4 in microglial cells exposed to FeSO4 and RSL3 using RT-qPCR (Figure 6D). The results showed a significant increase in the mRNA expression of TNF-α and ACSL4, confirming the successful establishment of a ferroptosis-induced inflammatory microglial model. Additionally, the elevated expression of SLC11A1 further validated our previous data analysis results. In addition, immunofluorescence staining demonstrated a significant increase in SLC11A1 protein expression in this model (Figure 6E), further supporting this finding at the protein level. To expand the evaluation of SLC11A1's diagnostic potential in other brain regions, we selected the prefrontal cortex expression dataset GSE33000 for ROC analysis (Figure 6F). The result showed that SLC11A1 exhibited fine diagnostic performance in the prefrontal cortex (AUC = 0.797, Sensitivity = 0.777, Specificity = 0.716). And DCA was utilized to assess the predictive performance of SLC11A1, the result indicated that in the probability threshold range of 25% to 85%, it demonstrated a higher net benefit, surpassing both full intervention and no intervention strategies (Figure 6G).

Discussion

AD is a progressive neurodegenerative disorder that typically affects the elderly population and is the most common form of dementia. In this study, we integrated bulk RNA-seq and scRNA-seq data to investigate the molecular changes in specific cells associated with inflammation and ferroptosis in AD, comparing brain and peripheral blood. This approach

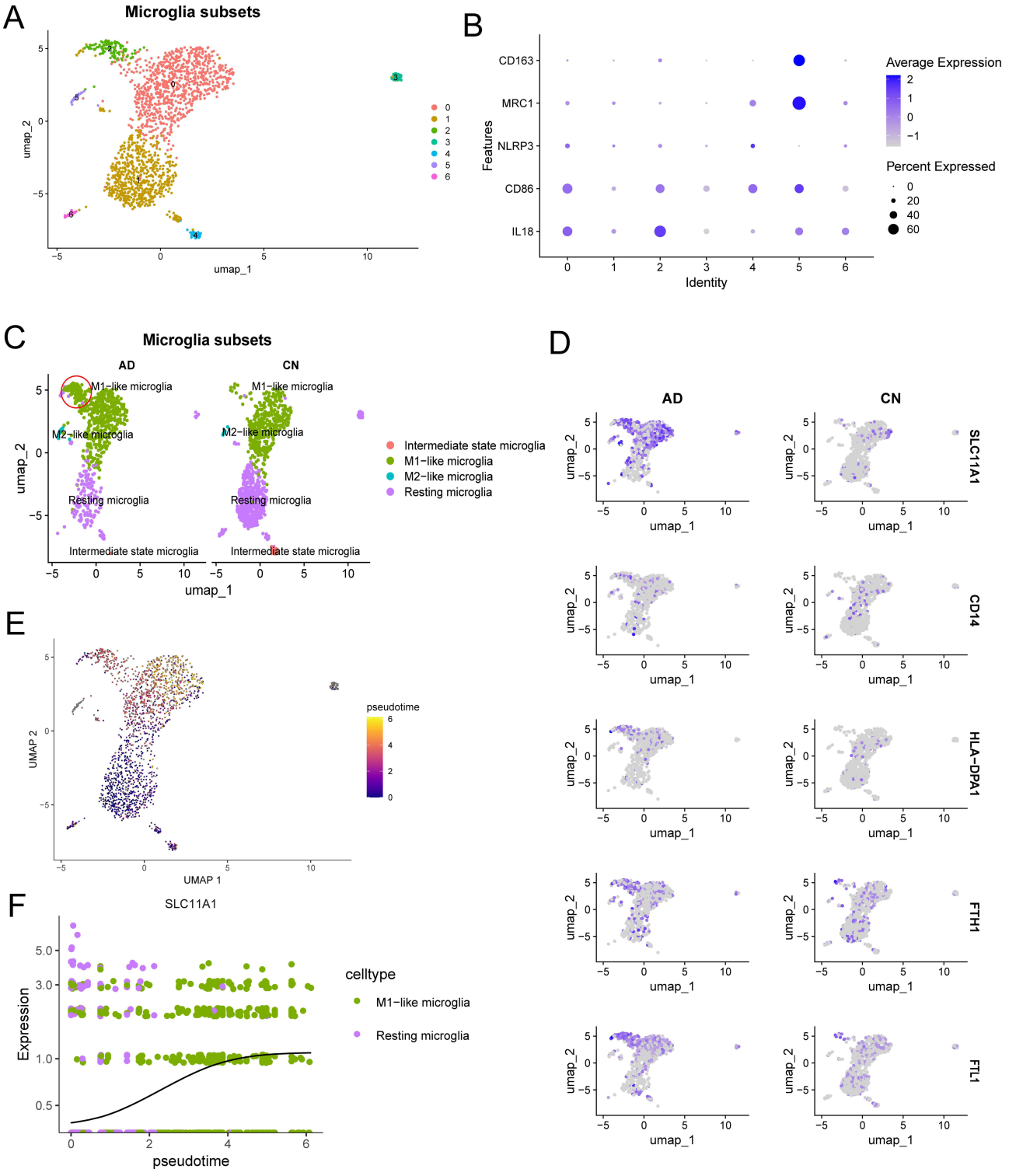

Figure 5 scRNA-seq data analysis of hippocampus microglia subpopulation. (**A-B**) Clustering of microglia and expression of their feature genes. (**C**) The distribution of microglia in AD and CN groups. (**D**) Expression distribution of related genes in different hippocampus microglia between AD and CN groups. (**E**) The diagram of cell differentiation at different periods, the bluer represents the differentiation at an earlier stage and the yellower represents the differentiation at a later stage. (**F**) Pseudotime analysis of SLC11A1 expression during the transition from resting-state microglia to the M1 phenotype.

Abbreviations: AD, Alzheimer's disease; CN, cognitively normal.

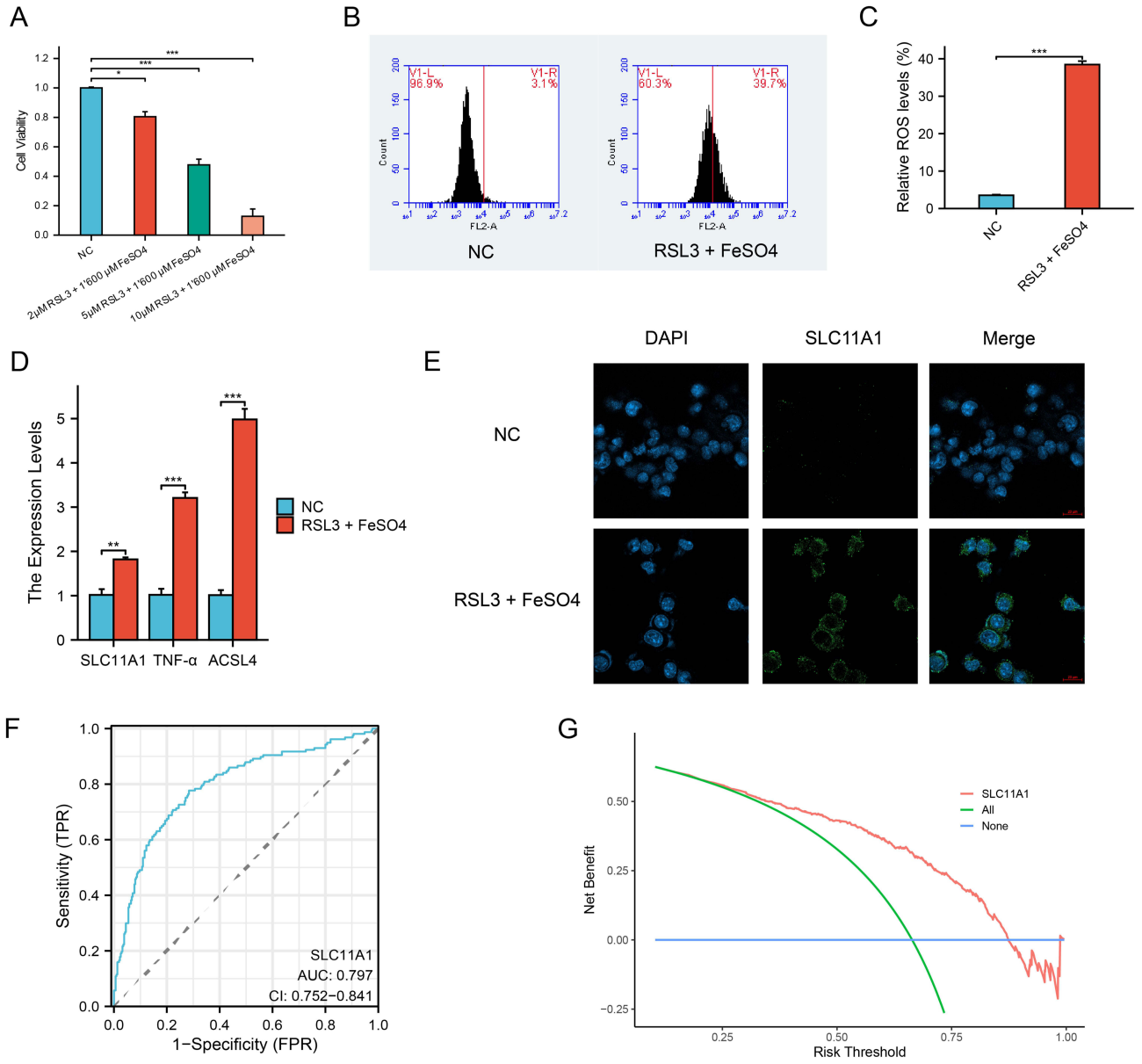

Figure 6 Vitro experiments validated SLC11A1 expression in the ferroptosis-induced inflammatory microglial model and the predictive performance of SLC11A1 based on ROC and DCA analyses. (**A**) Cell viability analysis in response to RSL3 and FeSO4 treatment. (**B**) Flow cytometry analysis of ROS levels, V1-R indicates the proportion of cells with elevated ROS levels. (**C**) Quantification of ROS levels in BV2 cells. (**D**) RT-qPCR detection of mRNA expression of SLC11A1, TNF-α and ACSL4 in Ferroptosis-induced inflammatory microglia. (**E**) Cellular immunofluorescence was used to detect the expression of SLC11A1 protein in Ferroptosis-induced inflammatory microglia. (**F**) ROC curve of SLC11A1 in the prefrontal cortex. (**G**) DCA of SLC11A1 Predictive Performance. The significance levels were indicated as follows: *p < 0.05, **p < 0.01, and ***p < 0.001. Statistical significance was determined using the *t*-test.

Abbreviations: ROS, Reactive oxygen species; RT-qPCR, reverse transcription quantitative polymerase chain reaction; ROC, receiver operating characteristic; DCA, decision curve analysis; NC, normal control.

helps establish links between cell function and gene expression, providing insights into the roles of these molecular pathways in the pathogenesis of AD.

The hippocampus not only plays a crucial role in memory formation and spatial navigation, but it is also a key site affected by AD.[34] In our study, we conducted a DEGs analysis using hippocampal expression data to explore molecular changes in the hippocampus of AD. Additionally, we performed WGCNA on this data and identified an AD-related gene module. We then intersected the DEGs and key module genes with inflammation-related genes sourced from GeneCards, resulting in the identification of a set of AD-related inflammatory genes. Biological process enrichment analysis of these genes revealed a strong link to inflammatory responses, as both wound healing and oxidative stress are closely tied to

https://doi.org/10.2147/JIR.S497418

inflammation. Notably, several of the enriched pathways, particularly those associated with oxidative stress, also overlap with ferroptosis, a regulated cell death process characterized by iron-dependent lipid peroxidation. The enrichment in focal adhesion and extracellular matrix remodeling further underscores potential roles of these genes in modulating inflammatory signaling and ferroptosis. Finally, hub genes were identified through PPI network analysis, providing deeper insights into their central roles in these processes.

Chronic neuroinflammation is a pathological feature of AD,[35] and cytokines such as interleukins (ILs) and tumor necrosis factor-alpha (TNF-α) are elevated in the brains of individuals with AD.[36] Recent studies have further suggested that this neuroinflammation may be closely associated with the infiltration of peripheral immune cells, such as monocytes and T cells, into the brain. These cells cross the BBB and enter the central nervous system, thereby exacerbating the inflammatory response and contributing to disease progression.[37] To explore this further, we used bulk RNA-seq data from the hippocampus of AD patients to evaluate immune cell infiltration through the ssGSEA method. The results showed significant differences in the infiltration of four immune cell types in the hippocampus of AD patients: activated CD4+ T cells, central memory CD4+ T cells, monocytes/macrophages, and eosinophils. Correlation analysis between the previously identified hub genes and these immune cell types identified four genes most strongly associated with them: C1S, CD44, SLC11A1, and ANXA2.

To further explore the connection between these four genes and the peripheral immune system in AD, we then analyzed their expression in peripheral blood, it is noteworthy that SLC11A1 not only shows significant differences in the brains of AD patients but also exhibits pronounced disparities in their peripheral blood. SLC11A1, formerly known as NRAMP1 (Natural Resistance-Associated Macrophage Protein 1), encodes a transmembrane protein belonging to the solute carrier family. It is involved in the transmembrane transport of divalent metal ions, such as iron and manganese. SLC11A1 protein is primarily expressed on the endoplasmic reticulum and lysosomal membranes of macrophages and neutrophils.[38] This protein plays a multifaceted role in macrophage activation, including inducing pro-inflammatory cytokines such as TNF-α, regulating MHC II expression, and generating ROS and reactive nitrogen intermediates, all of which are essential for the immune system's function.[39] This discovery led us to conduct an in-depth correlation analysis between SLC11A1 expression and the hallmark pathologies of AD in model mice. The results of this analysis revealed a strong correlation between SLC11A1 levels and the severity of both Aβ and Tau pathologies, suggesting a potential role of SLC11A1 in the progression of these pathological features. Furthermore, the GSEA results highlighted a significant association of SLC11A1 with pathways involved in antigen processing and presentation. This finding implies that SLC11A1 might influence the immune response in AD, particularly in the context of neuroinflammation, which is a critical aspect of AD pathology.

The subsequent hippocampal scRNA-seq analysis revealed that SLC11A1 was primarily expressed in microglia within the hippocampus, with its expression significantly upregulated in the AD group. Interestingly, similar findings were observed in the AD middle temporal gyrus, where SLC11A1 was prominently expressed in microglia and exhibited a comparable upregulation pattern. This suggests that the dysregulation of SLC11A1 in microglia may not be confined to the hippocampus but could represent a broader pathological feature across different brain regions associated with AD. Furthermore, in the peripheral blood environment, SLC11A1 was predominantly expressed in monocytes, showing significant upregulation in AD patients. This suggests that microglia expressing SLC11A1 in the AD brain may be linked to peripheral blood monocytes.

Microglial cells are resident macrophages in the CNS.[40] In a healthy CNS, they perform various functions, including clearing dead cells and other debris, supporting neuron health, and repairing damaged tissues.[41] The activation of microglia in the CNS is heterogeneous and can be categorized into two opposing types: M1 phenotype and M2 phenotype, with M1 phenotype having pro-inflammatory effects, while the M2 phenotype has anti-inflammatory and tissue repair functions.[42] We further extracted and integrated the hippocampal microglial subpopulations from both the AD and CN groups, followed by re-clustering analysis. This allowed us to more finely categorize the microglia into distinct states, including resting, intermediate, M1-like, and M2-like phenotypes. Our findings revealed that SLC11A1 was predominantly expressed in M1 microglia in the AD group, and pseudotime analysis indicates that SLC11A1 is associated with the polarization of microglia from a resting state to the M1 phenotype, indicating its potential role in promoting pro-inflammatory responses in AD pathology. Notably, we identified a distinct subpopulation within the M1

microglia of the AD group, characterized by the expression of monocyte markers such as CD14 and HLA-DPA1.[43] This suggests a potential peripheral origin of this subpopulation, as these markers are commonly associated with monocytes. The observed upregulation of SLC11A1 in both AD microglia and peripheral blood monocytes further supports the hypothesis of a dynamic interplay between peripheral immune cells and the CNS in AD. Furthermore, the high expression of FTH1 (ferritin heavy chain 1) and FTL1 (ferritin light chain 1), two essential genes involved in iron storage and metabolism, within this subpopulation provides additional insight into its potential functional role. FTH1 encodes the heavy chain subunit of ferritin, which possesses ferroxidase activity essential for converting Fe^{2+} to Fe^{3+}, thus facilitating safe iron storage and minimizing the generation of ROS through Fenton reactions.[44] FTL1, on the other hand, encodes the light chain subunit of ferritin, which is critical for stabilizing the ferritin complex and enhancing its capacity for iron sequestration, thereby contributing to the safe storage of excess iron and protection against iron-induced oxidative damage.[45]

Multiple sclerosis (MS) and AD are both common degenerative diseases of the central nervous system. The EAE model is widely used in MS research and simulates the inflammatory environment of the CNS, and studies have indicated a higher likelihood of co-occurrence between MS and AD.[46,47] This allows the EAE model to partially simulate the immune-mediated inflammatory processes observed in AD. Considering that the EAE model mimics chronic neuroinflammation by causing BBB damage and facilitating immune cell infiltration, we analyzed single-cell data from the brains of EAE model mice. And we successfully observed ferroptosis-associated microglial subpopulations, previously identified in AD, in the brains of EAE model mice. These microglial subpopulations also showed significant expression of SLC11A1, iron metabolism-related genes (such as FTH1 and FTL1), and the monocyte marker gene CD14. This suggests that ferroptosis-related immune responses may not be restricted to AD pathology but are a broader feature of central nervous system inflammation. Additionally, the CellChat analysis revealed that monocytes infiltrate associated microglia demonstrated robust intra-cellular and resident microglia interactions across various pathways, particularly involving chemokine (C-C motif), Tnf and C3 receptor-ligand pairs, and the unique presence of C3 receptor-ligand pairs in monocytes infiltrate associated microglia reflects their heterogeneity compared to resident microglia. Previous studies have reported that inhibiting C3 reduces the number of phagocytic microglia and the extent of early synaptic loss, which suggested these microglia's critical role in promoting inflammatory responses and regulating immune reactions.[48]

In the in vitro cell experiment, we used a combination of RSL3 and FeSO4 to stimulate BV2 microglial cells and induce an iron death-related inflammatory phenotype. The results showed that under this stimulation condition, ROS production in BV2 cells was significantly increased, and the RNA levels of TNF-α and ACSL4 were also significantly elevated. TNF-α is a key pro-inflammatory cytokine known to play an important role in neuroinflammation by activating signaling pathways such as NF-κB, which promotes the exacerbation of the inflammatory response.[49] ACSL4 is one of the key fatty acid synthases in the process of ferroptosis, promoting the accumulation of polyunsaturated fatty acids, which in turn accelerates lipid peroxidation, an important regulatory factor of ferroptosis.[50] Upregulation of ACSL4 expression exacerbates lipid peroxidation during ferroptosis and further promotes the occurrence of inflammation. Meanwhile, the RNA and protein levels of SLC11A1 were both upregulated in this cell model, indicating that SLC11A1 may play an important role in the process of ferroptosis. As an iron transporter, upregulation of SLC11A1 may enhance intracellular iron accumulation, thereby promoting lipid peroxidation and ROS generation, which drives the progression of ferroptosis. In addition, the increased expression of SLC11A1 may further promote microglial immune responses, enhancing the release of inflammatory factors and forming a positive feedback loop, ultimately exacerbating neuroinflammation and neurodegeneration. These results suggest that SLC11A1 not only plays a crucial role in ferroptosis but may also be involved in microglial-mediated inflammatory responses, making it a potential therapeutic target. Additionally, employing ROC curves and DCA with prefrontal cortex expression data further underscored the diagnostic potential of SLC11A1 in the prefrontal cortex. However, the specific mechanisms through which SLC11A1 influence AD still require further experimental exploration. This study also has some limitations. First, although we have revealed the potential role of SLC11A1 in AD through RNA sequencing and single-cell analysis, the lack of in vivo experiments and animal model validation, particularly with clinical sample data, is a limitation. Second, the specific mechanisms by which SLC11A1 influences iron metabolism and immune responses have not been thoroughly explored. Future research should further validate its function through gene editing and experimental models.

Conclusion

In conclusion, this study integrates bulk RNA-seq and single-cell RNA-seq data from AD patients and reveals that SLC11A1 is closely associated with inflammation related to ferroptosis in AD. We observed significant upregulation of SLC11A1 in microglia in the hippocampus and peripheral blood monocytes, highlighting the interaction between peripheral immune cells and the central nervous system. Additionally, the expression of SLC11A1 was elevated in a ferroptosis-induced microglial model, suggesting its potential involvement in ferroptosis. These findings provide new insights into the role of SLC11A1 in AD and may lay the groundwork for its use as a therapeutic target in AD.

Data Sharing Statement

Data used in this study are available from public databases and can be obtained from the corresponding author upon reasonable request.

Ethics Approval

According to Article 32, Items 1 and 2 of the "Measures for Ethical Review of Life Science and Medical Research Involving Human Beings" issued in China in 2023, research conducted using legally obtained public data, data generated through non-interfering observation of public behavior, or anonymized information data may be exempt from ethical review. This exemption aims to reduce unnecessary burdens on researchers and promote the development of life science and medical research involving human participants.

Acknowledgments

We thank the researchers for sharing the GEO dataset used in this study, as well as the creators of the public database.

Author Contributions

All authors have made substantial contributions to the manuscript, including the conception, study design, execution, data collection, analysis, and interpretation; participated in drafting, revising, or critically reviewing the article; approved the final version for publication; agreed to the submission of the manuscript to the specified journal; and take responsibility for all aspects of the work.

Funding

This work was supported by the National Natural Science Foundation of China (31900485) and grant from The Scientific Research Program of FuRong Laboratory (No. 2023SK2096).

Disclosure

The authors declare that they have no competing interests in this work.

References

1. Meyers EA, Sexton C, Snyder HM, et al. Impact of Alzheimer's association support and engagement in the AD/ADRD research community through the COVID-19 pandemic and beyond. *Alzheimers Dement*. 2023;19(7):3222–3225. doi:10.1002/alz.13015
2. Streit WJ, Phan L, Bechmann I. Ferroptosis and pathogenesis of neuritic plaques in Alzheimer's disease. *Pharmacol Rev*. 2024. doi:10.1124/pharmrev.123.000823
3. Sun Y, Chen P, Zhai B, et al. The emerging role of ferroptosis in inflammation. *Biomed Pharmacother*. 2020;127:110108. doi:10.1016/j.biopha.2020.110108
4. Beschorner R, Nguyen TD, Gözalan F, et al. CD14 expression by activated parenchymal microglia/macrophages and infiltrating monocytes following human traumatic brain injury. *Acta Neuropathol*. 2002;103(6):541–549. doi:10.1007/s00401-001-0503-7
5. Djukic M, Mildner A, Schmidt H, et al. Circulating monocytes engraft in the brain, differentiate into microglia and contribute to the pathology following meningitis in mice. *Brain*. 2006;129(Pt 9):2394–2403. doi:10.1093/brain/awl206
6. Ayka A, Şehirli AÖ. The Role of the SLC Transporters Protein in the Neurodegenerative Disorders. *Clin Psychopharmacol Neurosci*. 2020;18(2):174–187. doi:10.9758/cpn.2020.18.2.174
7. Li X, Yang Y, Zhou F, et al. SLC11A1 (NRAMP1) polymorphisms and tuberculosis susceptibility: updated systematic review and meta-analysis. *PLoS One*. 2011;6(1):e15831. doi:10.1371/journal.pone.0015831

8. Melia J, Lin R, Xavier RJ, et al. Induction of the metal transporter ZIP8 by interferon gamma in intestinal epithelial cells: potential role of metal dyshomeostasis in Crohn's disease. *Biochem Biophys Res Commun*. 2019;515(2):325–331. doi:10.1016/j.bbrc.2019.05.137
9. Jamieson SE, White JK, Howson JM, et al. Candidate gene association study of solute carrier family 11a members 1 (SLC11A1) and 2 (SLC11A2) genes in Alzheimer's disease. *Neurosci Lett*. 2005;374(2):124–128. doi:10.1016/j.neulet.2004.10.038
10. Salazar J, Mena N, Hunot S, et al. Divalent metal transporter 1 (DMT1) contributes to neurodegeneration in animal models of Parkinson's disease. *Proc Natl Acad Sci U S A*. 2008;105(47):18578–18583. doi:10.1073/pnas.0804373105
11. De Bastiani MA, Bellaver B, Carello-Collar G, et al. Cross-species comparative hippocampal transcriptomics in Alzheimer's disease. *iScience*. 2024;27(1):108671. doi:10.1016/j.isci.2023.108671
12. Wu Z, Dong L, Tian Z, et al. Integrative Analysis of the Age-Related Dysregulated Genes Reveals an Inflammation and Immunity-Associated Regulatory Network in Alzheimer's Disease. *mol Neurobiol*. 2024;61(8):5353–5368. doi:10.1007/s12035-023-03900-z
13. Xu M, Zhou H, Hu P, et al. Identification and validation of immune and oxidative stress-related diagnostic markers for diabetic nephropathy by WGCNA and machine learning. *Front Immunol*. 2023;14:1084531. doi:10.3389/fimmu.2023.1084531
14. Miller JA, Woltjer RL, Goodenbour JM, et al. Genes and pathways underlying regional and cell type changes in Alzheimer's disease. *Genome Med*. 2013;5(5):48. doi:10.1186/gm452
15. Yao Z, Dong H, Zhu J, et al. Age-related decline in hippocampal tyrosine phosphatase PTPRO is a mechanistic factor in chemotherapy-related cognitive impairment. *JCI Insight*. 2023;8(14). doi:10.1172/jci.insight.166306
16. Langfelder P, Horvath S. WGCNA: an R package for weighted correlation network analysis. *BMC Bioinf*. 2008;9:559. doi:10.1186/1471-2105-9-559
17. Yu G, Wang LG, Han Y, et al. clusterProfiler: an R package for comparing biological themes among gene clusters. *OMICS*. 2012;16(5):284–287. doi:10.1089/omi.2011.0118
18. Lin G, Li N, Liu J, et al. Identification of key genes as potential diagnostic biomarkers in sepsis by bioinformatics analysis. *PeerJ*. 2024;12:e17542. doi:10.7717/peerj.17542
19. Liu S, Meng Y, Zhang Y, et al. Integrative analysis of senescence-related genes identifies robust prognostic clusters with distinct features in hepatocellular carcinoma. *J Adv Res*. 2024;2024.
20. Wu Y, Liang S, Zhu H, et al. Analysis of immune-related key genes in Alzheimer's disease. *Bioengineered*. 2021;12(2):9610–9624. doi:10.1080/21655979.2021.1999553
21. Sood S, Gallagher IJ, Lunnon K, et al. A novel multi-tissue RNA diagnostic of healthy ageing relates to cognitive health status. *Genome Biol*. 2015;16(1):185. doi:10.1186/s13059-015-0750-x
22. Matarin M, Salih DA, Yasvoina M, et al. A genome-wide gene-expression analysis and database in transgenic mice during development of amyloid or tau pathology. *Cell Rep*. 2015;10(4):633–644. doi:10.1016/j.celrep.2014.12.041
23. Subramanian A, Tamayo P, Mootha VK, et al. Gene set enrichment analysis: a knowledge-based approach for interpreting genome-wide expression profiles. *Proc Natl Acad Sci U S A*. 2005;102(43):15545–15550. doi:10.1073/pnas.0506580102
24. Xue W, He W, Yan M, et al. Exploring shared biomarkers of myocardial infarction and Alzheimer's disease via single-cell/nucleus sequencing and bioinformatics analysis. *J Alzheimers Dis*. 2023;96(2):705–723. doi:10.3233/JAD-230559
25. Soreq L, Bird H, Mohamed W, et al. Single-cell RNA sequencing analysis of human Alzheimer's disease brain samples reveals neuronal and glial specific cells differential expression. *PLoS One*. 2023;18(2):e0277630. doi:10.1371/journal.pone.0277630
26. Xiong LL, Xue LL, Du RL, et al. Single-cell RNA sequencing reveals B cell-related molecular biomarkers for Alzheimer's disease. *Exp Mol Med*. 2021;53(12):1888–1901. doi:10.1038/s12276-021-00714-8
27. Fournier AP, Tastet O, Charabati M, et al. Single-cell transcriptomics identifies brain endothelium inflammatory networks in experimental autoimmune encephalomyelitis. *Neurol Neuroimmunol Neuroinflamm*. 2023;10(1). doi:10.1212/NXI.0000000000200046
28. Zhang X, Lan Y, Xu J, et al. CellMarker: a manually curated resource of cell markers in human and mouse. *Nucleic Acids Res*. 2019;47(D1):D721–D728. doi:10.1093/nar/gky900
29. Jean-Baptiste K, McFaline-Figueroa JL, Alexandre CM, et al. Dynamics of gene expression in single root cells of Arabidopsis thaliana. *Plant Cell*. 2019;31(5):993–1011. doi:10.1105/tpc.18.00785
30. Sui X, Zhang R, Liu S, et al. RSL3 drives ferroptosis through GPX4 inactivation and ROS production in colorectal cancer. *Front Pharmacol*. 2018;9:1371. doi:10.3389/fphar.2018.01371
31. Ryan SK, Zelic M, Han Y, et al. Microglia ferroptosis is regulated by SEC24B and contributes to neurodegeneration. *Nat Neurosci*. 2023;26(1):12–26. doi:10.1038/s41593-022-01221-3
32. Narayanan M, Huynh JL, Wang K, et al. Common dysregulation network in the human prefrontal cortex underlies two neurodegenerative diseases. *mol Syst Biol*. 2014;10(7):743. doi:10.15252/msb.20145304
33. Kohs T, Fallon ME, Oseas EC, et al. Pharmacological targeting of coagulation factor XI attenuates experimental autoimmune encephalomyelitis in mice. *Metab Brain Dis*. 2023;38(7):2383–2391. doi:10.1007/s11011-023-01251-1
34. Moreno-Jiménez EP, Flor-García M, Terreros-Roncal J, et al. Adult hippocampal neurogenesis is abundant in neurologically healthy subjects and drops sharply in patients with Alzheimer's disease. *Nat Med*. 2019;25(4):554–560. doi:10.1038/s41591-019-0375-9
35. Langworth-Green C, Patel S, Jaunmuktane Z, et al. Chronic effects of inflammation on tauopathies. *Lancet Neurol*. 2023;22(5):430–442. doi:10.1016/S1474-4422(23)00038-8
36. Swardfager W, Lanctôt K, Rothenburg L, et al. A meta-analysis of cytokines in Alzheimer's disease. *Biol Psychiatry*. 2010;68(10):930–941. doi:10.1016/j.biopsych.2010.06.012
37. Jorfi M, Maaser-Hecker A, Tanzi RE. The neuroimmune axis of Alzheimer's disease. *Genome Med*. 2023;15(1):6. doi:10.1186/s13073-023-01155-w
38. White JK, Stewart A, Popoff JF, et al. Incomplete glycosylation and defective intracellular targeting of mutant solute carrier family 11 member 1 (Slc11a1). *Biochem J*. 2004;382(Pt 3):811–819. doi:10.1042/BJ20040808
39. Blackwell M, Goswami T, Evans CA, et al. SLC11A1 (formerly NRAMP1) and disease resistance. *Cell Microbiol*. 2001;3(12):773–784. doi:10.1046/j.1462-5822.2001.00150.x
40. Martin E, El-Behi M, Fontaine B, et al. Analysis of microglia and monocyte-derived macrophages from the central nervous system by flow cytometry. *J Vis Exp*. 2017; 124. doi:10.3791/55781-v

41. Nayak D, Roth TL, McGavern DB. Microglia development and function. *Annu Rev Immunol*. 2014;32:367–402. doi:10.1146/annurev-immunol-032713-120240
42. Tang Y, Le W. Differential roles of m1 and m2 microglia in neurodegenerative diseases. *mol Neurobiol*. 2016;53(2):1181–1194. doi:10.1007/s12035-014-9070-5
43. Sferruzza G, Clarelli F, Mascia E, et al. Transcriptomic analysis of peripheral monocytes upon fingolimod treatment in relapsing remitting multiple sclerosis patients. *mol Neurobiol*. 2021;58(10):4816–4827. doi:10.1007/s12035-021-02465-z
44. Tian Y, Lu J, Hao X, et al. FTH1 inhibits ferroptosis through ferritinophagy in the 6-OHDA model of parkinson's disease. *Neurotherapeutics*. 2020;17(4):1796–1812. doi:10.1007/s13311-020-00929-z
45. Cao H, Zuo C, Huang Y, et al. Hippocampal proteomic analysis reveals activation of necroptosis and ferroptosis in a mouse model of chronic unpredictable mild stress-induced depression. *Behav Brain Res*. 2021;407:113261. doi:10.1016/j.bbr.2021.113261
46. Liu N, Yu W, Sun M, et al. Dabrafenib mitigates the neuroinflammation caused by ferroptosis in experimental autoimmune encephalomyelitis by up regulating Axl receptor. *Eur J Pharmacol*. 2024;973:176600. doi:10.1016/j.ejphar.2024.176600
47. Avitan I, Halperin Y, Saha T, et al. Towards a consensus on Alzheimer's disease comorbidity? *J Clin Med*. 2021;10(19):4360. doi:10.3390/jcm10194360
48. Hong S, Beja-Glasser VF, Nfonoyim BM, et al. Complement and microglia mediate early synapse loss in Alzheimer mouse models. *Science*. 2016;352(6286):712–716. doi:10.1126/science.aad8373
49. Lecca D, Jung YJ, Scerba MT, et al. Role of chronic neuroinflammation in neuroplasticity and cognitive function: a hypothesis. *Alzheimers Dement*. 2022;18(11):2327–2340. doi:10.1002/alz.12610
50. Cui J, Chen Y, Yang Q, et al. Protosappanin A protects dox-induced myocardial injury and cardiac dysfunction by targeting ACSL4/FTH1 axis-dependent ferroptosis. *Adv Sci*. 2024;11(34):e2310227. doi:10.1002/advs.202310227